BAYESIAN IMAGE SOURCE METHOD FOR GEOACOUSTIC INVERSION

Laurent Guillon French Naval Academy Research Center, BCRM Brest, CC 600, 29240 Brest cedex 9, France. laurent.guillon@ecole-navale.fr
Stan E. Dosso School of Earth and Ocean Sciences, University of Victoria, Victoria, British Columbia, V8W 3P6, Canada
N. Ross Chapman School of Earth and Ocean Sciences, University of Victoria, Victoria, British Columbia, V8W 3P6, Canada

1 INTRODUCTION

Knowledge of seafloor properties is important for many naval, environmental, geological, and geotechnical applications. Direct measurements, *in situ* or in laboratory on samples, provide knowledge of some physical parameters with a very good resolution. However, complimentary remote sensing techniques based on acoustics have some advantages: cost, coverage, automation. Different techniques have been developed: analysis of side-scan sonar or multibeam echosounder reflectivity maps, matched-field processing, analysis of scattered or reflected signals, passive acoustics, to list a few (see e.g. [1] or [2] and references therein).

The present work deals with a recent geoacoustic inversion technique, the Image Source Method (ISM), which provides the local sound-speed profile (SSP) of layered seafloors with good resolution and at a low computational cost [3–5]. The objective of this work is to develop a Bayesian inference approach for ISM to obtain not only a point estimate of the seabed SSP but their posterior probability density (PPD) which provides quantitative uncertainty estimates that take into account the modelling approximations and data uncertainties[1].

The remainder of this paper is organized in two sections. Section 2 presents the ISM along with its Bayesian extension. In section 3, the ISM results are presented for both synthetic data, and for experimental data acquired in a laboratory water tank where properties of the bottom are well known.

2 PRINCIPLES OF THE BAYESIAN IMAGE SOURCE METHOD

2.1 THE IMAGE SOURCE METHOD

The ISM is based on analysis of the reflection of a broadband acoustic signal emitted by a point source above a layered seafloor and recorded by a hydrophone array (Figure 1.a). Under some assumptions, particularly the Born approximation to neglect multiple reflections inside the sediment stack, the signal reflected by the layered seafloor can be modelled as being emitted by a set of image sources (IS), symmetric about the real source relative to the reflecting interfaces. Therefore, the layered seafloor can be represented by an equivalent system where the layer thicknesses are doubled and the IS are placed on the interfaces (Figure 1.b). In this system, the arrival angle and the travel time of the various arrivals are exactly the same as in the real configuration.

The locations of the IS are linked directly to the SSP of the layered seafloor, and the idea of the ISM is to detect and localize these IS from the recorded signals in order to infer the SSP. When the SSP is known, the IS are exactly below the source, placed on the interfaces, and their locations do not depend on the receiver positions since the refraction process is taken into account (Figure 1.b). But, in the context of geoacoustic inversion, the SSP is unknown. So, instead of dealing with the “real” IS, the

[1] Part of this paper is under review for the IEEE Journal of Oceanic Engineering [6]

recorded signals are modelled as being emitted by "virtual" IS representing the source positions that match the measured travel times and arrival angles at a hydrophone location if the entire medium is homogeneous water, i.e. when acoustic rays are straight lines. These virtual IS are no longer located on the interfaces, nor on the vertical axis below the source (Figure 1.c). Moreover, their positions depend on the receiver locations. Consequently, when the IS detection and location is performed with an array of N_h hydrophones, instead of having one receiver and one IS located by its arrival angle and travel time, we have N_h receivers and N_h virtual IS. To apply the inversion algorithm (described in the next paragraph), the multiple receivers and the multiple sources must each be merged into a single point. This merging process constitutes the approximation of the forward modelling of the ISM.

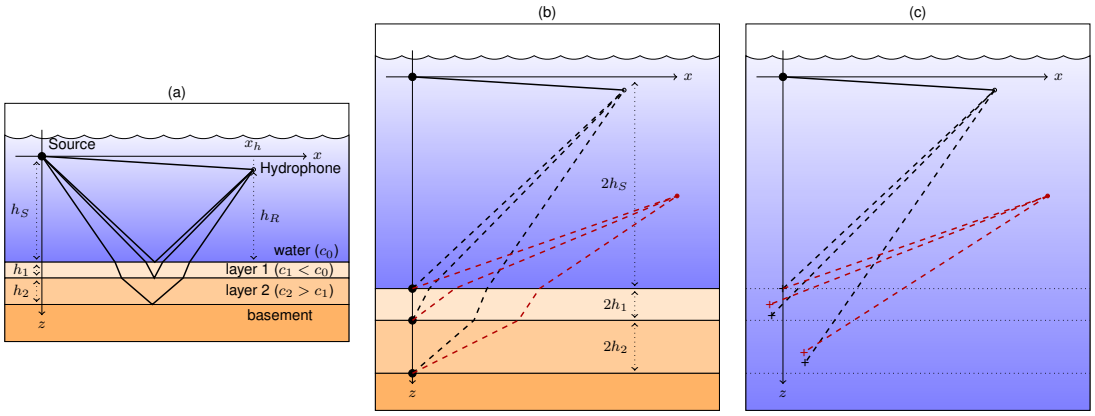

Figure 1: (a) Reflection of a point source signal by a 2-layer seafloor. (b) Modelling of this situation by image sources with refraction processes and reception at two different hydrophones (in black and red). (c) Modelling of this situation by virtual image sources when the seafloor is unknown.

The ISM is a two-step method (Figure 2). From the recorded signals, an algorithm is applied to detect and localize the IS. So far, three different algorithms have been developed for this task: the first one based on migration and semblance functions [4], the second one based on the Teager-Kaiser energy operator (TKEO) and a triangulation process [5], and the last one based on TKEO and a Bayesian formulation [6]. Once the IS are detected, their number gives directly the number of layers in the seafloor, with respect to the vertical resolution and the penetration depth of the acoustic data. For each IS, the algorithm gives its position by estimation of arrival angle and travel time. These two data for each layer are the inputs of the second step of the ISM, the inversion algorithm. This step is very simple [6] since it is only based on the Snell-Descartes law of refraction. The ISM requires some supplementary information, in particular a very good knowledge of the acquisition geometry.

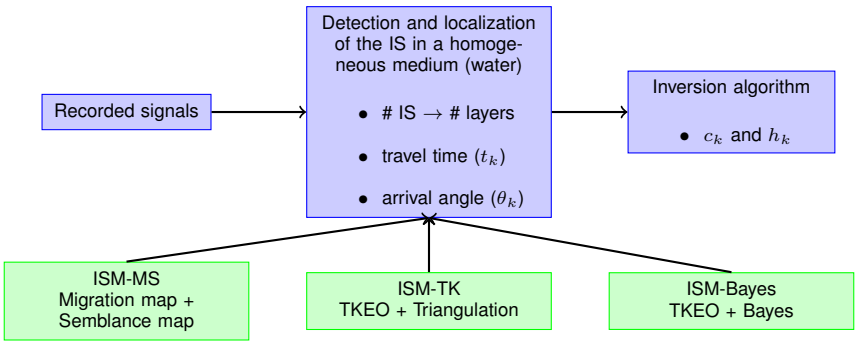

Figure 2: General structure of ISM, including the Bayesian ISM developed here.

2.2 THE BAYESIAN ISM

In this section, we explain the principle of the Bayesian version of the ISM, later referred to as BISM for Bayesian-ISM. We consider that the arrival times are detected for each recorded signal and therefore

the travel times are known by the knowledge of emission time from the source. In practice and in the examples described in the next section, this is done with TKEO [5].

The starting point of the BISM here is to consider that we are seeking the median position (x, z) of virtual IS of a particular layer i and that $t_k^{(i)}$ with $k \in [1..N_h]$ are the travel times between the hydrophones and this median position. The virtual IS are defined in a homogeneous medium with sound speed c_0; hence, these travel times are converted directly into distances $d_k^{(i)}$. In the following, we omit the superscripts (i) for convenience. The model parameters to be determined are the coordinates of the virtual IS: $\mathbf{m} = (x, z)$. The data are the travel times: $\mathbf{d} = t_k$ with $k \in [1..N_h]$.

The forward model $\mathbf{d} = g(\mathbf{m})$ is simply solved by the following system of equations:

$$t_k = g_k(x, z) = \frac{1}{c_0}\sqrt{(x - X_k)^2 + (z - Z_k)^2}\,, \tag{1}$$

with $k \in [1..N_h]$ and where X_k and Z_k are the coordinates of the hydrophones.

The objective is to obtain the posterior probability density (PPD) expressed in Bayes' theorem:

$$P(\mathbf{m}|\mathbf{d}) = \frac{P(\mathbf{d}|\mathbf{m})P(\mathbf{m})}{P(\mathbf{d})}\,. \tag{2}$$

Once the experiment has been carried out and the data obtained, $P(\mathbf{d})$ is a constant factor which can be absorbed into the normalization and the probability density function (PDF) $P(\mathbf{d}|\mathbf{m})$ can be identified as a function of $\mathbf{m}$ known as the likelihood function. If we assume that the errors on the data are independent and Gaussian distributed with standard deviation σ_t, this likelihood function can be written as :

$$L(x, z) \propto \exp\left[-\frac{1}{2\sigma_t^2}\sum_{k=1}^{N_h}\left(t_k^{cal}(x, z) - t_k^{obs}\right)^2\right]\,, \tag{3}$$

where the calculated travel times t_k^{cal} are obtained by the forward model and the observed travel times t_k^{obs} by applying the TKEO detection algorithm to recorded acoustic time series.

By construction, the virtual IS are located around the vertical axis below the real source. To define a relatively uniformative prior, the prior PDF $P(\mathbf{m})$ is set to a uniform probability distribution within a box surrounding this vertical axis.

The PPD $P(\mathbf{m}|\mathbf{d})$ is obtained through the Metropolis-Hastings sampling algorithm (see e.g. [7] or [8]). This gives N_{samp} samples of the PPD consistent with equation (2). From each pair of (x, z) taken in the PPD samples, the SSP is estimated from the algorithm presented in the previous section yielding a sampled PPD for the SSP. In this procedure, lower and upper bounds are set on $\tilde{c}$ and $\tilde{e}$ in order to avoid unrealistic SSP. Finally, a median SSP can be computed from the set of PPD samples.

3 RESULTS

3.1 SYNTHETIC DATA

The BISM is first applied to synthetic data computed by the software specfem2D[2] which is a spectral element code developed to simulate seismic-wave propagation at the Earth scale [9]. Recently, this software has been applied to underwater acoustics problems [10] and to T-wave generation and propagation modeling [11].

The specfem2D configuration which was used to produce these acoustic data includes a source at 12 m above floor level, an array with 15 hydrophones and an inter-sensor distance equal to 1 m, the first hydrophone being 24 m from the source. The use of a towed source and a horizontal array

[2]This software is available at: http://geodynamics.org/cig/software/specfem2d/

instead of using a moored vertical array [3] allows the ISM to invert for range-dependent seafloors [4]; however, that is not considered here.

The seafloor in the example consists of 2 layers, each 2 m thick, with sound speeds of 1650 m/s and 1750 m/s above a semi-infinite basement of 1800 m/s. The densities of each layer are set to realistic values according to classical empirical relationships [1].

In order to test the sensitivity of BISM to the acquisition geometry, we run simulations on two different array shapes. The first one is sinusoidal with 20 cm amplitude and 12.5 m wavelength, and the second one is inspired from a realistic array shape [12] (Figure 3).

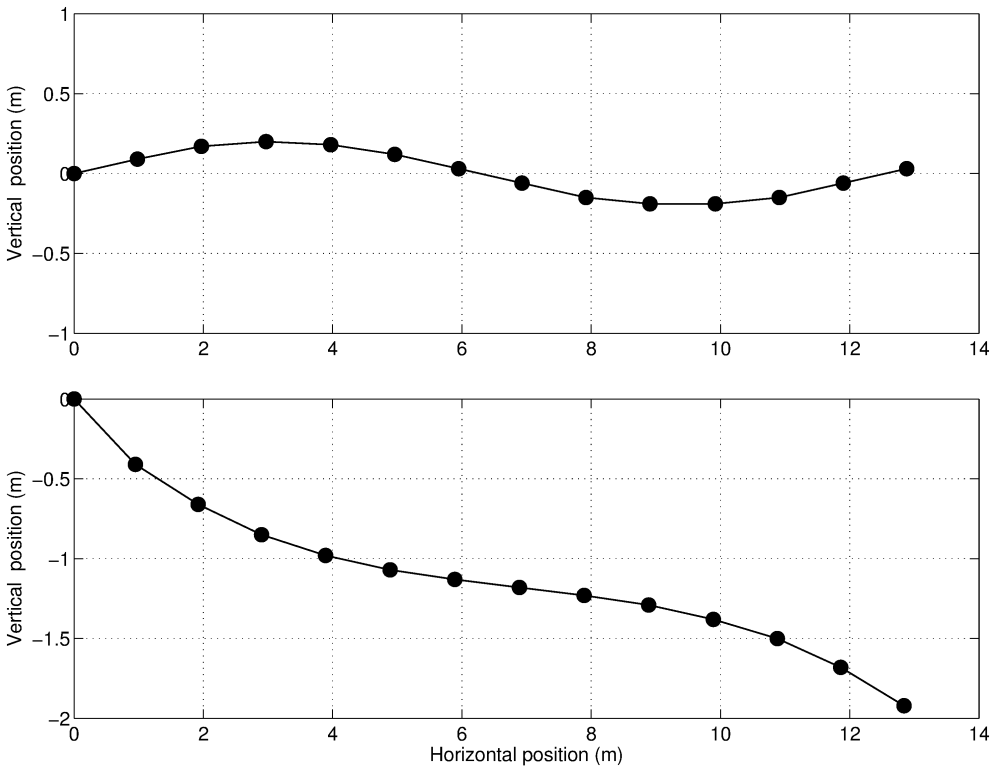

Figure 3: Array shapes used in the simulations: (top) sinusoidal array, (bottom) realistic array shape.

The results obtained by BISM are computed for the two cases with two strategies each: first, we run BISM knowing the hydrophone positions, and second, we assume that we do not know these positions and we suppose that the array is straight. In all cases, we assume that the standard deviation of the measured arrival times is equal to 5 time samples. The results obtained are shown in Figures 4 and 5 and lead to the following observations. First, if the acquisition geometry is perfectly known, the BISM provides a very good estimates of the seafloor SSP. Moreover, it includes the modelling approximations and data uncertainties to provide the PPD of the estimated parameters which is important to quantify the information content of the ISM and uncertainties of the SSP estimates. The BISM results are very similar to those obtained by other inversion techniques based on travel times [13] but with reduction in computational time of at least a factor of ten [6]. The second conclusion is that the knowledge of the acquisition geometry is essential to BISM. Indeed, the results obtained assuming that the array is straight are significantly biased compared to the true parameter values. This dependence on knowledge of the array geometry is not specific to BISM, but is common to almost all geoacoustic inversion methods. However, the Bayesian approach applied here quantifies this dependence, and it will be useful in future work to address this issue.

Some techniques have already been developed to correct the array shape before performing geoacoustic inversion [4, 14]. They are based on the measurement of the direct and first reflected arrival times. Depending on the water depth, the surface reflected path may also be used to this purpose.

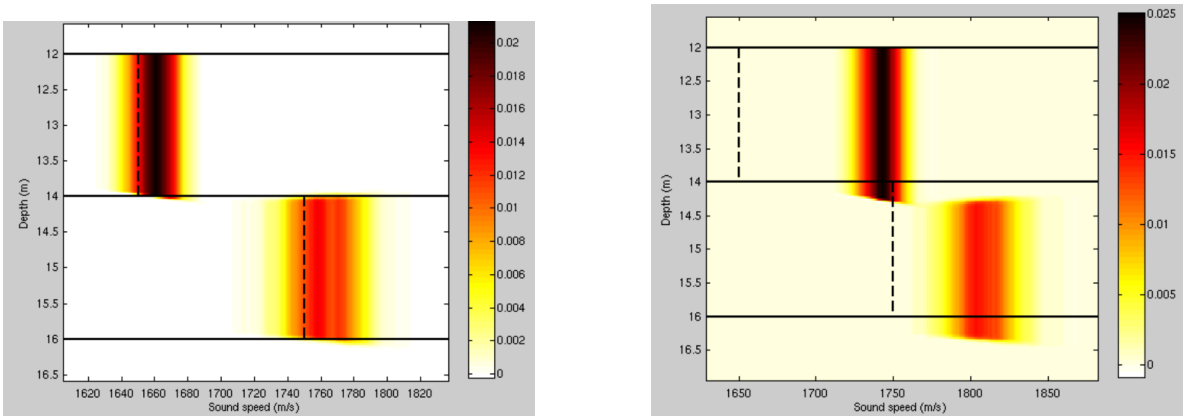

Figure 4: PPD of the SSP obtained by BISM in first case (sinusoidal array): (left) when the array shape is known, and (right) when the array is supposed straight.The horizontal black lines represent the position of the interfaces and the vertical dashed lines represent the true sound speeds.

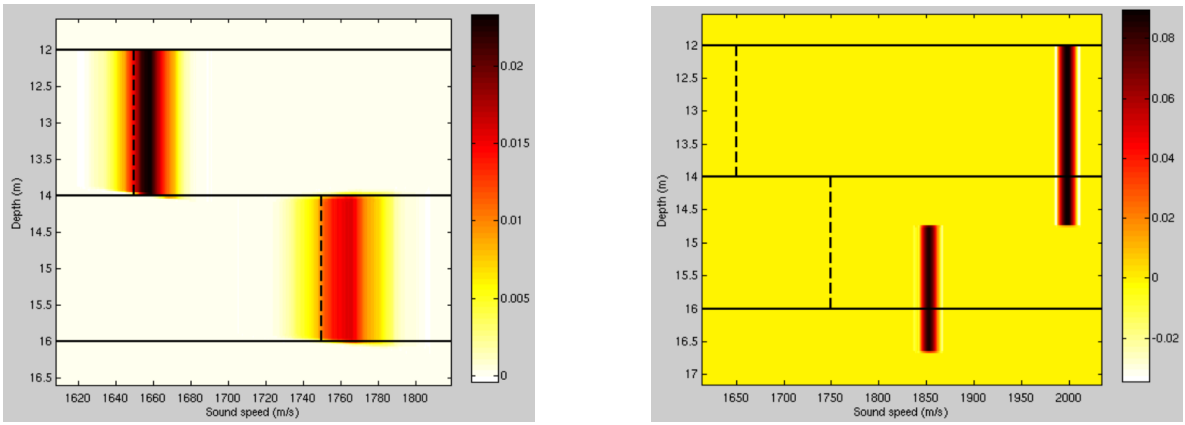

Figure 5: PPD of the SSP obtained by BISM in second case (realistic array): (left) when the array shape is known, and (right) when the array is supposed straight. The horizontal black lines represent the position of the interfaces and the vertical dashed lines represent the true sound speeds.

3.2 TANK DATA

The second test case is the application of BISM to acoustic data acquired in a water tank with synthetic plates on the bottom to mimic a layered seafloor. This experiment was conducted at ISEN (Institut Supérieur de l'Electronique et du Numérique), a French engineering school located in Brest. It was designed to test the ISM on real data acquired in a controlled environment and the data were used to invert the density of the plates with an improvement of ISM [15].

The tank was 3 m $\times$ 2 m with a water depth of 1 m (Figure 6 left). It was equipped with 2 metal arms immersed in water, each arm having 3 degrees of freedom, three translations and one rotation, that were enabled by step by step motors. Each arm supported a B&K broadband transducer: one as the source and the other as one element of a receiving array. The array was synthesized by moving the receiver and repeating the experiment. The temperature was measured continuously to provide the water sound speed.

The two plates at the bottom of the tank (Figure 6 right) were 50 cm wide, 50 cm long and of different thicknesses (Table 1). The first plate was made of Teflon, and the second of resin. The geoacoustic parameters of the plates are displayed in Table 1 where the densities were estimated from measured weights and volumes and the sound speeds came from the literature.

The signal probe used for the experiment was a pure sine wave centred at 150 kHz and sampled at

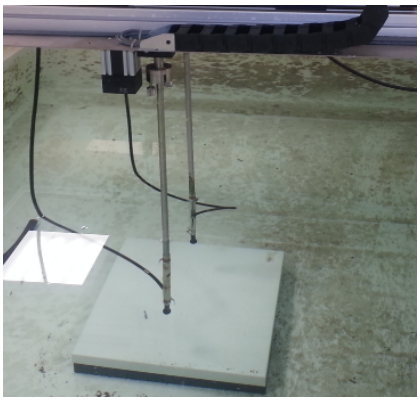

Figure 6: Left: water tank at ISEN. Right: synthetic plates in the tank

Material	ρ (g/cm^3)	c (m/s)	h (cm)
Teflon	2.178	$\simeq$ 1450	4.35
Resin	1.928	$\simeq$ 2000	4.47

Table 1: Geoacoustic parameters of the plates

800 kHz with duration of 6.6 μs. In order to estimate accurately the time delay of the received pulse the acquisition task was perfectly synchronized with the generated wave by using a digital trigger provided by the acquisition card (National Instrument card PCI-6115). The impulse response (IR) of the system was obtained after a Wiener deconvolution of the recorded signals (Figure 7).

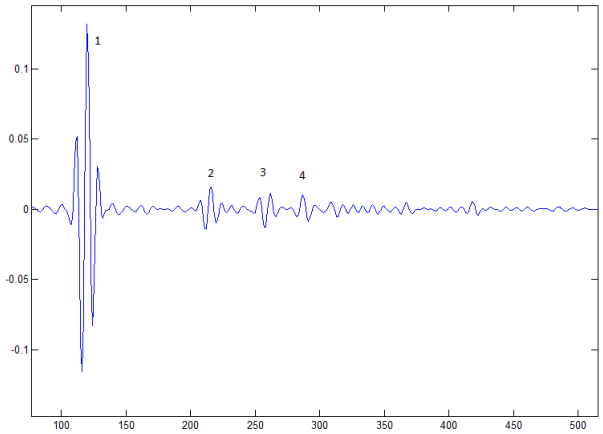

Figure 7: IR of the system at one hydrophone location. The numbers show the different acoustic paths: direct (1), reflections at the first (2) and second (3) plates, and reflection at the interface between the 2nd plate and tank bottom (4). The time is displayed in sample numbers and the vertical axis has arbitrary units.

Although the geometry is known with very good accuracy, the hydrophones positions are corrected by applying the procedure described in [14]. The BISM is then applied to the IR recorded at each hydrophone position. The PPD of the SSP is displayed in Figure 8.

The results are satisfactory. The PPD is quite broad but centred at the “true” sound speeds. The thicknesses are well estimated. Considering the frequency used here, the layers are roughly four wavelengths thick which appears to be enough for good estimation.

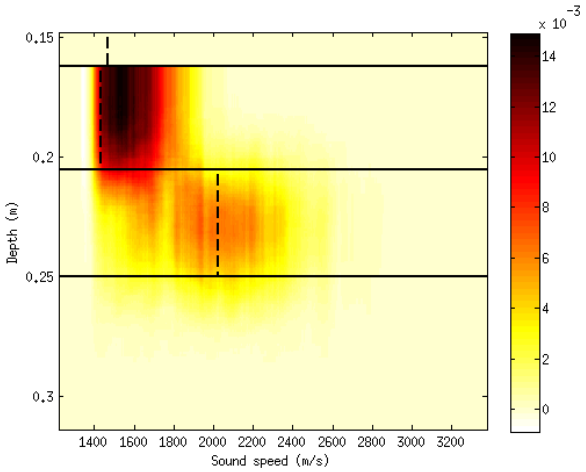

Figure 8: PPD of the SSP obtained by BISM on data acquired in water tank. The horizontal black lines represent the position of the interfaces and the vertical dashed lines represent the sound speeds found in the literature.

4 CONCLUSION

The ISM and its Bayesian extension have been presented in this paper and applied on both synthetic and real data. The results show that this method has several advantages: it is conceptually easy to understand, straightforward to compute, and it has a low computational cost, at least for the basic version. The BISM slows down the computational speed but it provides an estimate of the PPD of the SSP which is important in geoacoustic inversion processes.

REFERENCES

1. D. Jackson and M. Richardson. *High-frequency seafloor acoustics*. Springer, 2007.
2. X. Lurton. *An introduction to underwater acoustics*. Springer, 2 edition, 2010.
3. S. Pinson and L. Guillon. Sound speed profile characterization by the image source method. *J. Acoust. Soc. Am.*, 128(4): pp. 1685–1693, 2010.
4. S. Pinson, L. Guillon, and C. Holland. Range dependent sediment sound speed profile measurements using the image source method. *J. Acoust. Soc. Am.*, 134(1): pp. 156–165, 2013.
5. A. Drira, L. Guillon, and A. Boudraa. Image source detection for geoacoustic inversion by the teager-kaiser energy operator. *J. Acous. Soc. Am. Express Letter*, : pp. EL258–EL264, 2014.
6. L. Guillon., S. E. Dosso, N. R. Chapman, and A. Drira. Bayesian geoacoustic inversion with the image source method. *IEEE J. Ocean. Eng.*, 2015. submitted.
7. K. Mosegaard and A. Tarantola. Probabilistic approach to inverse problems. In *International handbook of earthquake and engineering technology*. Academic press, 2002.
8. S. E. Dosso and M. J. Wilmut. Uncertainty estimation in simultaneous bayesian tracking and environmental inversion. *J. Acoust. Soc. Am.*, 124(1): pp. 82–97, 2008.
9. D. Komatitsch and J. P. Vilotte. The spectral-element method: an efficient tool to simulate the seismic response of 2d and 3d geological structures. *Bull. Seismol. Soc. Am.*, 88(2): pp. 368–392, 1998.
10. P. Cristini and D. Komatitsch. Some illustrative examples of the use of a spectral-element method in ocean acoustics. *J. Acoust. Soc. Am.*, 131(3): pp. EL229–EL235, 2012.

11. G. Jamet, C. Guennou, L. Guillon, C. Mazoyer, and J.-Y. Royer. T-wave generation and propagation: A comparison between data and spectral element modeling. *J. Acoust. Soc. Am.*, 134(4): pp. 3376–3385, 2013.

12. B. Howard. Calculation of the shape of a towed underwater acoustic array. *IEEE J. Ocean. Eng.*, 17(2): pp. 193–203, 1992.

13. J. Detmer, S. E. Dosso, and C. W. Holland. Uncertainty estimation in seismo-acoustic reflection travel time inversion. *J. Acoust. Soc. Am.*, 122: pp. 161–176, 2007.

14. A. Drira, L. Guillon, and A. Boudraa. Estimation de la forme d'une antenne d'hydrophone a l'aide de l'operateur d'energie de teager-kaiser. In *CFA (Congres Francais d'Acoustique) 2014*, pp. 731–736, 2014. in French.

15. A. Drira, Y. Mével, P.-J. Bouvet, L. Guillon, and A. Boudraa. Estimation of density of a stratified seafloor with the image source method: validation by tank experiments. In L. Bjorno and J. Papadakis, eds., *3rd Underwater Acoustics Conference and Exhibition*, Chania, Greece, 2015.